

## Roles of Aconitase in Growth, Metabolism, and Morphological Differentiation of *Streptomyces coelicolor*

P. H. VIOLLIER,<sup>1</sup>† K. T. NGUYEN,<sup>1</sup> W. MINAS,<sup>2</sup> M. FOLCHER,<sup>1</sup> G. E. DALE,<sup>1</sup>‡  
AND C. J. THOMPSON<sup>1</sup>\*

Department of Molecular Microbiology, Biozentrum, University of Basel, Basel,<sup>1</sup> and  
Institute of Biotechnology, ETH-Zürich, HPT, Zürich,<sup>2</sup> Switzerland

Received 6 September 2000/Accepted 8 February 2001

**The studies of aconitase presented here, along with those of citrate synthase (P. H. Viollier, W. Minas, G. E. Dale, M. Folcher, and C. J. Thompson, *J. Bacteriol.* 183:3184–3192, 2001), were undertaken to investigate the role of the tricarboxylic acid (TCA) cycle in *Streptomyces coelicolor* development. A single aconitase activity (AcoA) was detected in protein extracts of cultures during column purification. The deduced amino acid sequence of the cloned *acoA* gene constituted the N-terminal sequence of semipurified AcoA and was homologous to bacterial A-type aconitases and bifunctional eukaryotic aconitases (iron regulatory proteins). The fact that an *acoA* disruption mutant (BZ4) did not grow on minimal glucose media in the absence of glutamate confirmed that this gene encoded the primary vegetative aconitase catalyzing flux through the TCA cycle. On glucose-based complete medium, BZ4 had defects in growth, antibiotic biosynthesis, and aerial hypha formation, partially due to medium acidification and accumulation of citrate. The inhibitory effects of acids and citrate on BZ4 were partly suppressed by buffer or by introducing a citrate synthase mutation. However, the fact that growth of an *acoA citA* mutant remained impaired, even on a nonacidogenic carbon source, suggested alternative functions of AcoA. Immunoblots revealed that AcoA was present primarily during substrate mycelial growth on solid medium. Transcription of *acoA* was limited to the early growth phase in liquid cultures from a start site mapped *in vitro* and *in vivo*.**

Members of the genus *Streptomyces* are spore-forming gram-positive soil bacteria having a developmental program that coordinates changes in growth rate, metabolism, and morphology (reviewed in references 7 and 20). After germination, during the first growth phase (39), these filamentous organisms generate a dense multicellular network within the nutrient substrate (22, 36). Biomass accumulation then slows down transiently; resumption of growth is coordinated with formation of antibiotics and aerial hyphae (13, 39). Acidification of glucose-based minimal medium, which occurs during early growth, is followed by a cyclic AMP-dependent metabolic switch that neutralizes the medium (39) and thus allows differentiation and antibiotic biosynthesis.

Developmental mutants have been isolated that are unable to erect aerial mycelium (bald), a phenotype often accompanied by defects in antibiotic biosynthesis. Many bald genes are homologous to known regulatory elements; however, the developmental functions they control are largely unknown. Evidence that certain bald genes are parts of an organized developmental system comes from complementation tests involving physiological interactions or exchange of signals between pairwise combinations of *bld* mutants. When two mutants are grown adjacent to each other, one of the pair is able to restore the ability of its neighbor to erect aerial hyphae (28, 29, 44, 45).

The fact that this response is partner dependent suggests a model in which complementation groups represent an ordered signaling cascade leading to aerial mycelium erection (28, 29, 44, 45).

Whereas many bald mutants are acidogenic on glucose-based media (39, 42), they are able to differentiate and remain neutral on mannitol-based media (39, 42). This may relate to their defects in catabolite repression (32) and accumulation of organic acids (39, 42). Therefore, carbon source and tricarboxylic acid (TCA) metabolism may play a central role in growth and development. In the accompanying article, we report that a mutant lacking the first enzyme of the TCA cycle, citrate synthase (CitA), is bald and does not produce antibiotics on glucose-containing media (42). *citA* could be placed between *bldJ* and *bldK* in the proposed signaling cascade.

The second enzyme of the TCA cycle, aconitase (EC 4.2.1.3), catalyzes the reversible isomerization of citrate to isocitrate (via *cis*-aconitate). In prokaryotes, aconitases have been most thoroughly studied in gram-negative bacteria, where they define two principal families (AcnA and AcnB) (14), sometimes present in the same organism. The AcnA- and AcnB-type aconitases in *Escherichia coli* are differentially regulated, suggesting separate physiological roles (9).

The recent discovery of novel biological roles and regulatory activities for aconitase suggested its possible alternative function in iron metabolism and mediating the bacterial oxidative stress response (1, 41). AcnA and AcnB in *Escherichia coli*, CitB (1), the only aconitase of *Bacillus subtilis*, and bifunctional eukaryotic aconitases (iron regulatory proteins) (33) contain an iron-sulfur center that senses low iron concentrations and oxidative stress. In response to these conditions, they bind to sequence motifs within mRNAs called iron regulatory ele-

\* Corresponding author. Mailing address: Biozentrum, University of Basel, Department of Molecular Microbiology, Klingelbergstrasse 70, CH-4056 Basel, Switzerland. Phone: 41 61 267 2116. Fax: 42 61 267 2118. E-mail: charles-j.thompson@unibas.ch.

† Present address: Department of Developmental Biology, Stanford University School of Medicine, Stanford, CA 94305-5329.

‡ Present address: Morphochem, Basel, BS 4058, Switzerland.

ments (IRE) and thereby provide posttranscriptional control of gene expression. This activity may play a role in bacterial differentiation and virulence. In *Legionella pneumophila* and *Xanthomonas campestris*, AcnA-type aconitases maintain iron homeostasis important for pathogenicity (27, 46). The fact that an enzymatically inactive aconitase (CitB) able to bind mRNA promoted sporulation in *B. subtilis* indicated its alternative role in development (1).

*citB* transcription is activated preceding sporulation (10) in response to citrate accumulation. In addition to its activity in relieving catabolite repression of *citB* expression (12, 30), citrate is a strong chelator of divalent cations needed as cofactors for the Spo0A phosphorelay system that initiates spore formation. Since both *citB* mutations and starvation for one of these divalent cations ( $Mn^{2+}$ ) arrest initiation of development at a comparable stage, Craig and coworkers have proposed a unifying model in which citrate-mediated chelation of divalent metals impedes the activity of kinases within the Spo0A phosphorelay (8). This concept is supported by the observation that an aconitase (*citB*)-citrate synthase (*citZ citA*) double mutant could overcome the block in expressing Spo0A-dependent genes in the *citB* mutant (19). Recently, Schwartz et al. (37) demonstrated that *Streptomyces viridochromogenes* has multiple aconitase activities, at least one of which is needed for normal morphologic differentiation.

Here we describe diverse physiological roles for *acoA*, a *Streptomyces coelicolor* aconitase gene that encodes the primary vegetative aconitase. Our results show that inactivation of *acoA* results in growth and developmental defects related to medium acidification, citrate accumulation, and possibly an alternative function of aconitase.

## MATERIALS AND METHODS

**Bacterial strains and media.** *E. coli* XL1-Blue (Stratagene) was used as the host for cloning. When *S. coelicolor* was transformed, nonmethylated DNA was prepared from *E. coli* ET 12567 (provided by D. MacNeil and T. MacNeil) in order to circumvent a restriction barrier (24). *E. coli* was grown in Luria broth supplemented, as required, with antibiotics purchased from Sigma: ampicillin (100  $\mu$ g/ml), kanamycin (50  $\mu$ g/ml), spectinomycin (100  $\mu$ g/ml), or apramycin (50  $\mu$ g/ml).

*S. coelicolor* MT1110 is a prototrophic, plasmid-free (SCP1<sup>-</sup> SCP2<sup>-</sup>) derivative of *S. coelicolor* A3(2) (15, 16, 39). Construction of the *citA* mutant BZ2 is described in the accompanying paper (42). For *S. coelicolor* growth curves in liquid media, 10 ml of a seed culture previously grown for at least 48 h (stationary phase) in YEME (16) served to inoculate 500 ml of YEME in a 2-liter baffled flask. This medium was supplemented with thiostrepton (5  $\mu$ g/ml), apramycin (20  $\mu$ g/ml), or spectinomycin (100  $\mu$ g/ml) as required. Solid complex media employed included R2YE, R5, MR5 (the same as R5 [16] except that glucose, sucrose, and proline were omitted). Minimal medium was based on MG (11) (maltose glutamate liquid medium containing 1.5% Difco agar) or SMMS (40) in which Casamino Acids were replaced by 0.5% asparagine. Test for auxotrophy were carried out on SMMS-based minimal medium (using 2% agarose [Sigma] instead of agar) with or without the addition of 50  $\mu$ g of glutamate/ml. These solid media were supplemented as required with antibiotics purchased from Sigma: thiostrepton (50  $\mu$ g/ml), apramycin (50  $\mu$ g/ml), or spectinomycin (500  $\mu$ g/ml).

**Media composition analyses.** To remove liquid from agar medium, contents of a plate were placed in a 30-ml tube, frozen at  $-80^{\circ}\text{C}$  for 1 h, thawed for 2 h at room temperature, and finally centrifuged at 20,000 rpm in an SS34 rotor. Ammonium concentrations were determined using the Dr. Lange LCK303 cuvette test in combination with the Dr. Lange CADAS 30 Photometer (Dr. Lange AG, Hegnau, Switzerland). The  $\text{NH}_4^+$  concentration was determined after a 30-min incubation at  $30^{\circ}\text{C}$ . Other metabolites (acetate, citrate, and pyruvate) were measured using enzyme-linked assays. Analyses were performed in an automatic enzymatic analyzer (Synchron CX5CE clinical system; Beckman In-

struments, Inc., Fullerton, Calif.). All tests are based on quantitative changes in NADH content reflected by changes in absorption at 340 nm. Commercial test kits were used to determine concentration of glucose (Beckman Synchron systems glucose reagent 442640; Beckman Instruments), acetate (TC acetic acid 148261; Roche Molecular Biochemicals, Basel, Switzerland), and citric acid (TC citric acid 139076; Roche). Pyruvate was assayed using standard protocols (2).

**Protein analyses.** Protein concentrations were determined by the Bradford technique (4) using a Bio-Rad kit and bovine serum albumin as a standard. Sodium dodecyl sulfate–10% polyacrylamide gel electrophoresis (SDS–10% PAGE) was performed as described by Laemmli (23). For immunoblots, crude cell lysates containing 20  $\mu$ g of protein were separated by SDS-PAGE. Proteins were transferred to a polyvinylidene difluoride (PVDF) membrane (Millipore) at 400 mA in 5 liters of transfer buffer (15 mM Tris, 120 mM glycine, 10% methanol) for 90 min. The membranes were incubated in blocking buffer (TBS [20 mM Tris-HCl, pH 7.6; 130 mM NaCl] containing 5% nonfat dried milk and 0.1% Tween 20) for 2 h at room temperature. The antibody raised against *E. coli* AcnA (kindly provided by John Guest) was added at a 1/10,000 dilution to the blocking buffer and incubated with the membrane for 1 h. Unbound antibody was removed by four 5-min washes in TBS. The membrane was immersed into blocking buffer containing horseradish peroxidase conjugated to swine anti-rabbit immunoglobulin G (Gibco) at a dilution of 1/10,000, incubated for 1 h, and then given four washes (5 min each) in TBS. AcnA cross-reacting bands were visualized by chemiluminescence (ECL Plus; Amersham Pharmacia).

Catechol dioxygenase (XylE) activities (18) in crude extracts were measured at  $37^{\circ}\text{C}$ , calculated as the rate of change in optical density at  $375\text{ nm min}^{-1}$ , and expressed as specific activity (units or milliunits per milligram of protein).

**Partial purification of AcoA.** Aconitase activity was assayed by measuring the conversion of isocitrate to *cis*-aconitate (43). All purification steps were performed at  $4^{\circ}\text{C}$  as rapidly as possible due to the lability of aconitase enzyme activity. *S. coelicolor* MT1110 mycelium (70 g [wet weight]) was lysed by sonication in 200 ml buffer A (20 mM Tris-HCl [pH 8.0], 0.1 mM dithiothreitol, 5% [vol/vol] glycerol) with 0.1 M NaCl supplemented with 1 mM citrate (to protect the enzyme) and complete protease inhibitors (Roche Molecular Biochemicals). Cell debris was removed by centrifugation at 15,000 rpm in a Sorvall GSA rotor. The supernatant was loaded onto a 50-ml Q-Sepharose Fast Flow column (XK26/20; Amersham Pharmacia) equilibrated in buffer A and eluted with a linear gradient from 0.1 to 1 M NaCl in buffer A. Active fractions were pooled, diluted in buffer A to give a conductivity equal to 0.1 M NaCl, and applied to an 8-ml Source Q column (XK16/20; Amersham Pharmacia) equilibrated in buffer A containing 0.1 M NaCl. The column was washed extensively, and adsorbed proteins were eluted using a linear gradient to 1 M NaCl in buffer A. Fractions that showed aconitase activity were collected and dialyzed against buffer P (50 mM  $\text{Na}_2\text{PO}_4\text{-Na}_2\text{HPO}_4$  [pH 7.5], 0.1 mM dithiothreitol, 5% [vol/vol] glycerol) containing 0.1 M NaCl and applied to an 8-ml Source S column (XK16/20; Amersham Pharmacia). Although this step contributed most to the purification, the enzyme activity was rapidly lost thereafter. After the aconitase activity was eluted from the cation exchanger with a linear gradient to 1 M NaCl in buffer P, the active fractions were concentrated by ultrafiltration (YM10; Amicon). The final purification step was achieved by gel filtration using a Superose 6 (Amersham Pharmacia) column equilibrated in buffer P containing 0.5 M NaCl, run at a flow rate of 0.5 ml/min. Fractions (1 ml) were assayed for aconitase activity and analyzed by SDS-PAGE.

**N-terminal amino acid sequencing of AcoA.** In order to determine the N-terminal sequence of the 97-kDa protein, 10  $\mu$ g was separated by SDS-PAGE, blotted onto a Millipore PVDF Immobilon membrane (using a buffer containing 10 mM CAPS [3-(cyclohexyl-amino)-1-propanesulfonic acid], pH 11, and 10% methanol), and subjected to Edman degradation.

**DNA techniques.** General DNA techniques were performed as described by Sambrook et al. (35). Minipreps and recovery of DNA fragments from agarose gels were done using Qiagen Qiaprep or Qiaquick systems.

**Cloning and sequencing of *acoA*.** *Taq* DNA polymerase (5 U; Roche Molecular Biochemicals) and the degenerate primers Aco3 (5'-G[G/C][G/C][C/T]GA T[A/G]TGGT[C/G/C]GT[G/C]GT-3') and Aco6 (5'-CC[G/C]CT[G/C]GT[G/C]GT[G/C]GC[G/C]TACG-3') were used in a PCR mixture (consisting of 100 pmol of both primers, 1  $\mu$ g of template DNA, 10% dimethyl sulfoxide, and 0.2 mM deoxynucleoside triphosphates in  $1\times$  PCR buffer supplemented with 0.15 mM  $\text{MgCl}_2$ ) to amplify a 381-bp fragment from MT1110 genomic DNA. This fragment was gel purified, blunt ended with T4 DNA polymerase, and cloned into the *EcoRV* site of pBluescript SK (Stratagene) to yield pVHP80.

After sequence confirmation that the PCR fragment contained a part of the aconitase gene (*acoA*), pVHP80 was digested with *Hind*III and *EcoRI* (flanking the *EcoRV* site in pBluescript SK) to generate a 381-bp fragment that was gel purified and labeled with  $[\alpha\text{-}^{32}\text{P}]\text{dATP}$  using random primers (Roche Molecular

Biochemicals). This probe identified a 7.2-kb band on Southern blots of *Bam*HI-digested *S. coelicolor* MT1110 genomic DNA. *Bam*HI genomic fragments were size fractionated on agarose gels to enrich for this fragment and ligated into *Bam*HI-digested pK18. An *acoA*-carrying plasmid (pVHP81) was identified by colony hybridization. pVHP84 was constructed by isolating a 3.6-kb *Nde*I/*Bam*HI fragment from pVHP81, treating the fragment with T4 DNA polymerase, and ligating it into *Eco*RV-cut pBluescript SK.

Sequencing was done on an ABI 373 sequencer (PE Applied Biosystems) using dye terminator cycle sequencing ready reactions (PE Applied Biosystems) according to the manufacturer's instructions. Standard universal and reverse primers were used to sequence the exonuclease III-deletion derivatives of pVHP84. Gaps were closed using *acoA*-specific primers. Sequences were assembled and analyzed with the aid of the Lasergene package (DNA Star).

**Operon fusion constructs with the *acoA* upstream region.** The *P<sub>acoA</sub>* region (a 277-bp *Xmn*I/*Nsi*I fragment containing 269 bp upstream of *acoA*) was subcloned in order to make operon fusions to the promoterless *xyIE* gene on the SCP2-derived shuttle vector pIJ2839 (constructed from pXE3 [18] by T. Clayton). This fragment was isolated from pVHP84, blunt ended with T4 DNA polymerase, and ligated into *Eco*RV-digested pBluescript SK to give pVHP85. The *Nsi*I/*Xmn*I fragment of pVHP85 containing *P<sub>acoA</sub>* was excised by *Hind*III (within the poly-linker)/*Bam*HI and cloned into similarly restricted pIJ2839, yielding pVHP171.

**Plasmids used to disrupt *S. coelicolor* *acoA*.** pVHP184 was made by amplifying a 1.1-kb fragment from pVHP84 using primers Aco12 (5'-AAGGAATTCGGCGGACCCGAACAAGATCAA-3') and Aco14 (5'-CTTCGAATTCAGGCC GTTCTCGACCGCCTTCTT-3') and *Taq* DNA polymerase (5 U; Roche Molecular Biochemicals), digesting it with *Eco*RI (site is underlined), and cloning it into pKC1132 (containing the apramycin resistance gene). pVHP185 was constructed in a similar manner using Aco13 (5'-CCCGAATTCCTCGGTCGACGACGAGACGCTGAA-3') and Aco15 (5'-GAAGAATTCGCTGTAGGACTTG GAGAACA-3') as primers to amplify a 1-kb *acoA* internal fragment from pVHP184. The PCR fragment amplified by Aco13 and Aco15 primers was also cloned into pSET151 (containing the thiostrepton resistance gene) to generate pVHP186.

**Disruption of *acoA* and complementation.** MT1110 protoplasts were transformed with pVHP184 or pVHP185 extracted from the nonmethylating *E. coli* strain ET12567. After 18 h incubation at 30°C, regeneration plates were flooded with 1 ml of a solution containing 1 mg of apramycin/ml. Two apramycin-resistant transformants having the correct insertion of the plasmid gave a PCR product of about 2 kb (BZ3) or 3 kb (BZ4). BZ5, an *acoA* *citA* double mutant, was derived from BZ2 (*citA*) (see the accompanying paper [42]) by insertional mutagenesis using pVHP186. The constructions were also confirmed by PCR and Southern blotting.

The integrative plasmid pPM925 (38) was used as a vector to complement the *acoA* lesion. pPM925 mediates insertion of cloned DNA into *Streptomyces* chromosomes at its pSAM2 attachment site. The 3.8-kb insert of pVHP84 was released by digestion with *Kpn*I and *Bam*HI and ligated into pPM925, yielding pPM925-*acoA*. pPM925-*acoA* or pPM925 was introduced into BZ4 by conjugation (26), selecting for thiostrepton- and apramycin-resistant exconjugants.

**Mapping transcriptional initiation sites.** In vitro transcription experiments were performed as described previously (6), and products were analyzed on 6% polyacrylamide-7 M urea gels.

RNA extracted from *S. coelicolor* MT1110 using hot phenol (25) was treated with RNase-free DNase I (Roche Molecular Biochemicals). One picomole of oligonucleotide that had been kinase labeled at the 5' end was used to prime cDNA synthesis from 10 µg of total RNA isolated from cultures grown in YEME to early exponential phase (10 h). The extension reaction was carried out for 1 h at 42°C using Superscript II reverse transcriptase (Gibco BRL).

**Purification of *S. coelicolor* RNA polymerase.** Total RNA polymerase (RNAP) was isolated from *S. coelicolor* MT1110 as described previously (5), with one modification: after the polymin P extractions and subsequent ammonium sulfate precipitation, heparin Sepharose chromatography was used instead of DNA cellulose chromatography. The sample was loaded onto a 25-ml heparin Sepharose Cl-6B (Amersham Pharmacia) column equilibrated in TGED buffer (0.1 M Tris-HCl [pH 7.9], 5% [vol/vol] glycerol, 0.1 mM EDTA, 0.1 mM dithiothreitol) containing 0.15 M NaCl. The column was washed extensively with TGED containing 0.2 M NaCl, and RNAP was step eluted with TGED containing 1 M NaCl. The eluate was dialyzed in TGED to a final salt concentration of 0.1 M NaCl and then applied to an 8-ml Source 15Q column (Amersham Pharmacia) equilibrated with the same buffer. After a washing step with TGED containing 0.2 M NaCl, RNAP was eluted with an 80-ml linear gradient of TGED buffer containing 0.7 M NaCl. One-milliliter fractions were collected and analyzed by SDS-PAGE. Fractions containing RNAP were identified by their  $\alpha$  and  $\beta\beta'$  subunits stained with Coomassie brilliant blue. Fifty-microliter samples of each

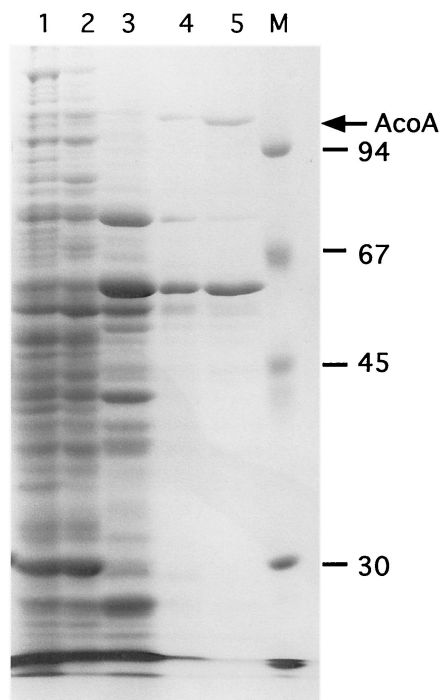


FIG. 1. Partial purification of AcoA from *S. coelicolor* crude extracts. *S. coelicolor* crude extract (lane 1) was fractionated by Q-Sepharose anion-exchange chromatography (lane 2), Source Q anion-exchange chromatography (lane 3), Source S cation-exchange chromatography (lane 4), and Superose 6 gel filtration chromatography (lane 5). Representative samples from each chromatographic step were resolved by SDS-PAGE and stained with Coomassie brilliant blue. The molecular masses of the protein marker present in lane M are indicated on the right (in kilodaltons). The arrow on the right designates the position of AcoA.

fraction containing RNAP were combined to yield the RNAP mixed holoenzymes that were used in the subsequent experiments.

**Nucleotide sequence accession number.** The fragment of *S. coelicolor* genomic DNA containing *acoA* has been deposited in GenBank under accession number AF180948.

## RESULTS

**Isolation of AcoA, the primary *S. coelicolor* aconitase.** The major aconitase activity detected in *S. coelicolor* protein extracts (AcoA) was partially purified using an ordered series of ion-exchange (Q-Sepharose, Source Q, and Source S) and gel filtration (Superose 6) chromatography steps (see Materials and Methods). The most active fraction from the Superose 6 column contained only two major proteins (100 and 62 kDa) detected by SDS-PAGE (Fig. 1). All known prokaryotic aconitases are large monomeric enzymes with predicted molecular masses of approximately 100 kDa. The N-terminal sequence of the 100-kDa protein obtained by Edman degradation was NH<sub>2</sub>-X-A-N-X-F-D-A-R-X-T (X represents an unassigned amino acid).

Only one aconitase activity peak was detected throughout purification, suggesting that it served as the primary enzyme in vivo. However, aconitases are characteristically unstable (21) (their [4Fe-4S] cluster is readily oxidized) and major losses of activity were observed during purification. Therefore, in vitro

activity may not be a reliable measure of relative *in vivo* function, and these data did not rule out the possibility that another undetected aconitase played the primary metabolic role. Genetic analyses were used to address this question.

**Isolation of the gene encoding AcoA.** To isolate the *acoA* gene, degenerate primers based on amino acids from two conserved regions of the AcoA family of aconitases (P-L-V-V-A-Y and T-D-H-I-S-P-A) allowed amplification of a 381-bp DNA fragment. This PCR fragment was used to probe Southern blots of *Bam*HI-digested *S. coelicolor* genomic DNA. The hybridizing 7.2-kb fragment was cloned and a 3.2-kb region containing *acoA* was sequenced (all subsequent references to nucleotide positions are with respect to this sequence). The sequence (nucleotides 340 to 3053) encoded a protein (904 amino acids) highly homologous to aconitases of *S. viridochromogenes* (PID g6456849; 91% identity), *Mycobacterium tuberculosis* (PID g3261503; 65% identity) and *Mycobacterium avium* (PID g3121732; 65% identity), *Corynebacterium glutamicum* (PID g4587326; 65% identity), and *X. campestris* (PID g2661438; 55% identity). The protein's predicted molecular mass of 97 kDa and pI of 4.7 were in good agreement with the mass measured on SDS-PAGE gels (100 kDa), and its N-terminal sequence was indistinguishable from that of purified AcoA. The corresponding open reading frame (ORF) initiated at a GTG translational initiation site that was preceded by a purine-rich sequence (GAAGGAGA) that could serve as a ribosome-binding site. These data indicated that the ORF encoded AcoA.

**Construction and morphology of *S. coelicolor acoA* mutants.** *acoA* mutants were constructed to investigate the possible role of aconitase in primary metabolism and growth, colonial development, or secondary metabolism. Repeated attempts to construct a stable mutant by a double-crossover event designed to replace *acoA* with an allele containing a resistance gene were unsuccessful. Disruption of the gene was achieved by insertion of plasmids containing internal fragments of *acoA*, via a single-crossover event. Two different ca. 1-kb fragments within the *acoA* ORF were amplified by PCR and cloned into plasmid pKC1132 (3) (generating pVHP184 and pVHP185; see Materials and Methods). Since pKC1132 is unable to replicate in *Streptomyces* spp., stable maintenance is most likely to occur by a single homologous recombination event between the cloned DNA and the *acoA* chromosomal locus. Apramycin-resistant colonies (BZ3 and BZ4, transformed with pVHP184 and pVHP185, respectively) were isolated. PCR and Southern hybridizations confirmed that integration events in BZ3 and BZ4 had disrupted the *acoA* gene (described in Materials and Methods). Immunoblots showed that the AcoA band was missing in BZ4 (see below).

BZ3 and BZ4 had similar phenotypic defects on R2YE. Both formed small colonies and produced little pigment or aerial hyphae even after prolonged incubation (BZ4 is shown in Fig. 2A and B). Introduction of the integrative plasmid containing the *acoA* locus (pPM925-AcoA) restored BZ4 (Fig. 2C, sector 2) to its wild-type parental colonial phenotype (Fig. 2C, sector 4; BZ3 was not tested). This proved that the phenotypes observed were due to *acoA* disruption and not to polar effects on downstream genes.

The phenotypes of the *acoA* mutants were highly unstable. To maintain the mutant allele, they were grown on media containing apramycin. Without this selection, apramycin-sen-

sitive strains appeared at high frequency, a phenomenon visualized as colonial sectors presumably reflecting a reversal of the integration event. Suppressor strains also appeared in the presence of apramycin, albeit at lower frequency (Fig. 2C, sector 2). Since these strains having wild-type morphology still had the plasmid inserted at the *acoA* locus (confirmed by PCR), they probably resulted from suppressive mutations that occurred elsewhere in the chromosome. Thus, the *acoA* mutants BZ3 and BZ4 could be reliably maintained only by frequent purification of small, bald, apramycin-resistant colonies on R2YE agar.

**Effect of the *acoA* mutation on flux through the TCA cycle.** Metabolic flux through the TCA cycle not only serves as the optimal aerobic pathway for the generation of ATP and reducing compounds but also supplies ketoglutarate for the biosynthesis of glutamate. Therefore, the immediate physiological consequences of the lack of aconitase could include the arrest of the TCA cycle leading to accumulation of the AcoA substrate (citrate) and glutamate auxotrophy.

BZ4 could not grow on minimal medium in the absence of glutamate. This was the first proof that metabolic flow through the TCA cycle was severely disrupted and that the protein encoded by *acoA* was the primary vegetative aconitase.

This was reconfirmed by analyses of the acids accumulated by the *acoA* mutant (BZ4) growing on glucose. MT1110 and BZ4 utilized glucose at about the same rate (Fig. 3B). While the wild type did not produce detectable amounts of citrate, BZ4 accumulated it continuously; levels had reached 14 mM and were increasing at 120 h (Fig. 3D). This provided direct physiological evidence that *acoA* encoded the aconitase with primary importance in oxidizing glucose via the TCA cycle. The accumulation of acetic acid and pyruvate in the medium (Fig. 3E and F) provided further evidence that TCA-based oxidative metabolism was blocked in the *acoA* mutant. Acetic acid is commonly produced from pyruvate by bacteria growing on glucose under oxygen-limited conditions when TCA cycle activity is minimal. During the course of development, wild-type MT1110 did not accumulate acetate (Fig. 3E).

**Dissecting the underlying causes of the growth defect of an *acoA* mutant.** The above results suggested that the *acoA* mutant defects might relate to pH, citrate accumulation, or alternative functions of aconitase.

In wild-type MT1110 cultures growing on cellophane disks overlying R2YE (which contains 25 mM TES buffer), the medium pH gradually decreased during substrate mycelial growth from its initial pH of 7.2 to 6.0 at 44 h and then increased during later stages of development (Fig. 3C). White aerial hyphae appeared around 30 h, red pigment appeared at 44 h, and gray spores appeared at 72 h (Fig. 3A). This biphasic pH change associated with aerial hyphae and pigment formation on R2YE was observed only when the strain was growing on cellophane disks (i.e., it was not observed in the accompanying study, where cultures were grown directly on the agar surface [42]). The phenomenon was similar to that observed on a glucose minimal medium (39).

In contrast, BZ4 lawns irreversibly acidified the medium to pH 3.5 (Fig. 3C). Medium acidification to pH values of <5 inhibits *S. coelicolor* growth and differentiation (39). Only very high concentrations of buffer (100 mM TES, designated R2YE-HITES) allowed maintenance of neutral pH. Even un-

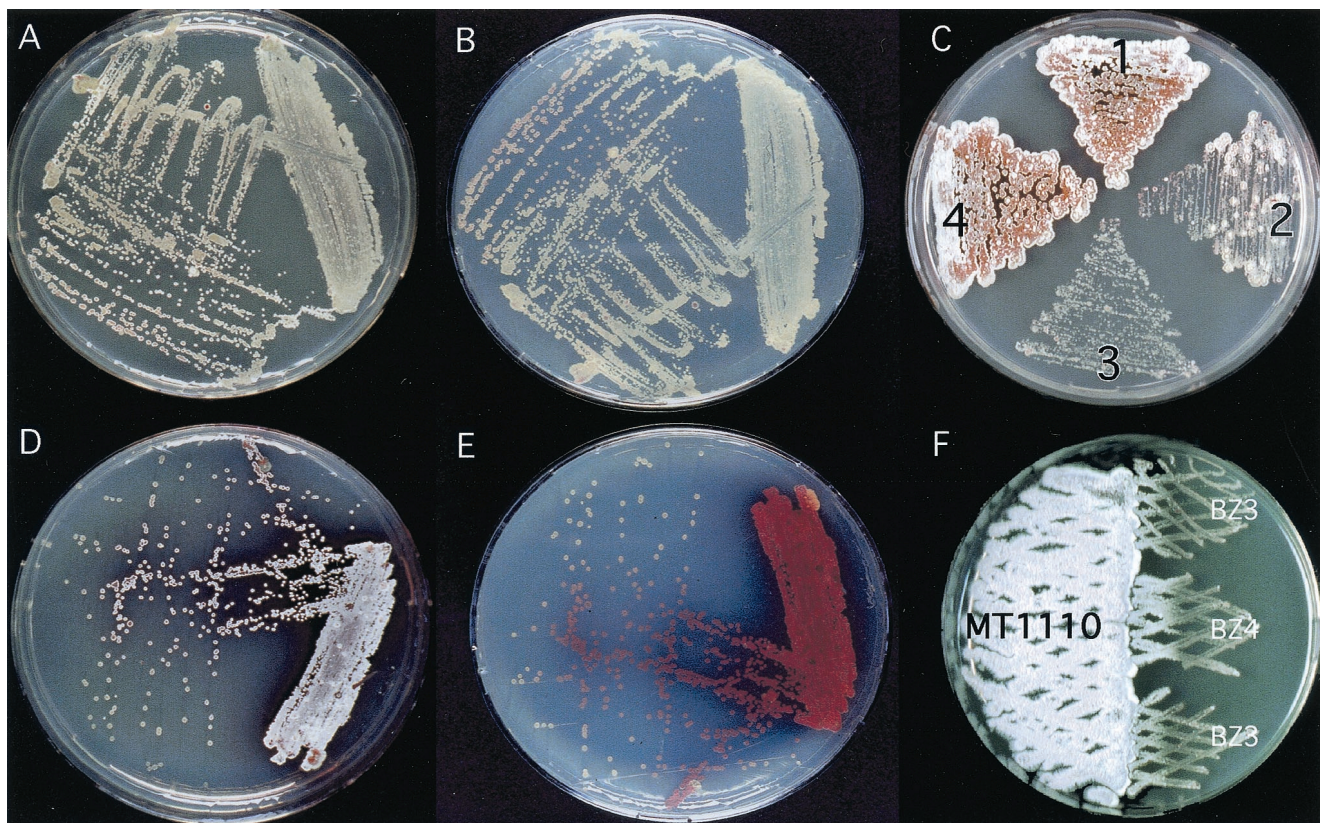


FIG. 2. Colonial morphology of the *acoA* mutant. The developmental processes of the *acoA* mutant, BZ4, was conditionally blocked on R2YE plates. BZ4 grew slowly and produced few white aerial hyphae (shown best in panel A, the top view) or pigmented antibiotics (shown best in panel B, the bottom view). When the medium was supplemented with 100 mM TES buffer, BZ4 colonies grew more rapidly but were still growth impaired compared to the wild type and were able to produce characteristic aerial mycelium (panel D, top view) and pigments (panel E, bottom view). Plate C illustrates complementation of the mutated *acoA* allele in BZ4: sector 1, MT1110; sector 2, BZ4; sector 3, BZ4/pPM925; sector 4, BZ4/pPM925-*acoA*. Note the appearance of several BZ4 revertants on plate C, sector 2. Developmental defects were also suppressed by growing either *acoA* mutant (BZ3 or BZ4) next to MT1110 (F). Since all plates had to be supplemented with 100  $\mu$ g of apramycin/ml to maintain the mutant *acoA* allele, MT1110 was transformed with a plasmid conferring resistance (pKC1218).

der these conditions, the *acoA* mutant was growth retarded; however, after prolonged cultivation (10 to 14 days), colonial development was clearly accelerated on R2YE-HITES, especially within densely seeded areas of the plate (Fig. 2D and E). Single, well-isolated colonies remained bald, indicating that plating density was a factor contributing to the conditional developmental defects.

In order to determine whether the *acoA* mutant phenotypes were specifically related to aconitase rather than reflecting a defect due to impaired TCA metabolism or citrate accumulation, an *acoA* mutant (BZ4) was compared to a citrate synthase mutant (BZ2) (Fig. 4). The mutant colonies displayed similar retardation in growth and differentiation on media containing glucose. In addition, on nonacidogenic plates containing mannitol instead of glucose, the *citA* mutant grew and differentiated normally; the *acoA* mutant was defective in growth but able to differentiate after prolonged incubation. This indicated that, in addition to acidogenesis, the *acoA* mutant had other growth defects.

Pleiotropic effects of aconitase mutants have been attributed partially to chelation of divalent cations by citrate that may limit the activity of enzymes and regulatory components de-

pendent on divalent cations (19, 41). Since these effects can be prevented by inactivation of the citrate synthase genes (19, 41), a *citA acoA* double mutant was constructed. *citA*, *acoA*, and *citA acoA* mutants were all growth inhibited on the acidogenic glucose-based medium (Fig. 4). Although the *citA* mutants grew like the wild type on mannitol, the *acoA* mutant remained severely growth inhibited. However, the *acoA* defect was partially suppressed in the *citA acoA* mutant; after long incubation, the double mutant grew into larger colonies than the *acoA* single mutant. Citrate was thus implicated as a second of at least three factors contributing to the growth defect of the *acoA* mutant.

In principle, chelator activity of citrate might be suppressed by supplementing the medium with appropriate concentrations of specific cations. However, the addition of various concentrations (1 to 100 mM) of  $\text{CuSO}_4$ ,  $\text{MnSO}_4$ , or  $\text{FeSO}_4$  did not visibly restore growth or development of BZ4 colonies on R2YE medium. Similarly, application of these heavy metals in solution (1 to 100 mM) to the surface of R2YE seeded with BZ4 did not accelerate growth or development (data not shown). These negative results were difficult to interpret. Citrate has a variable affinity for a variety of essential divalent

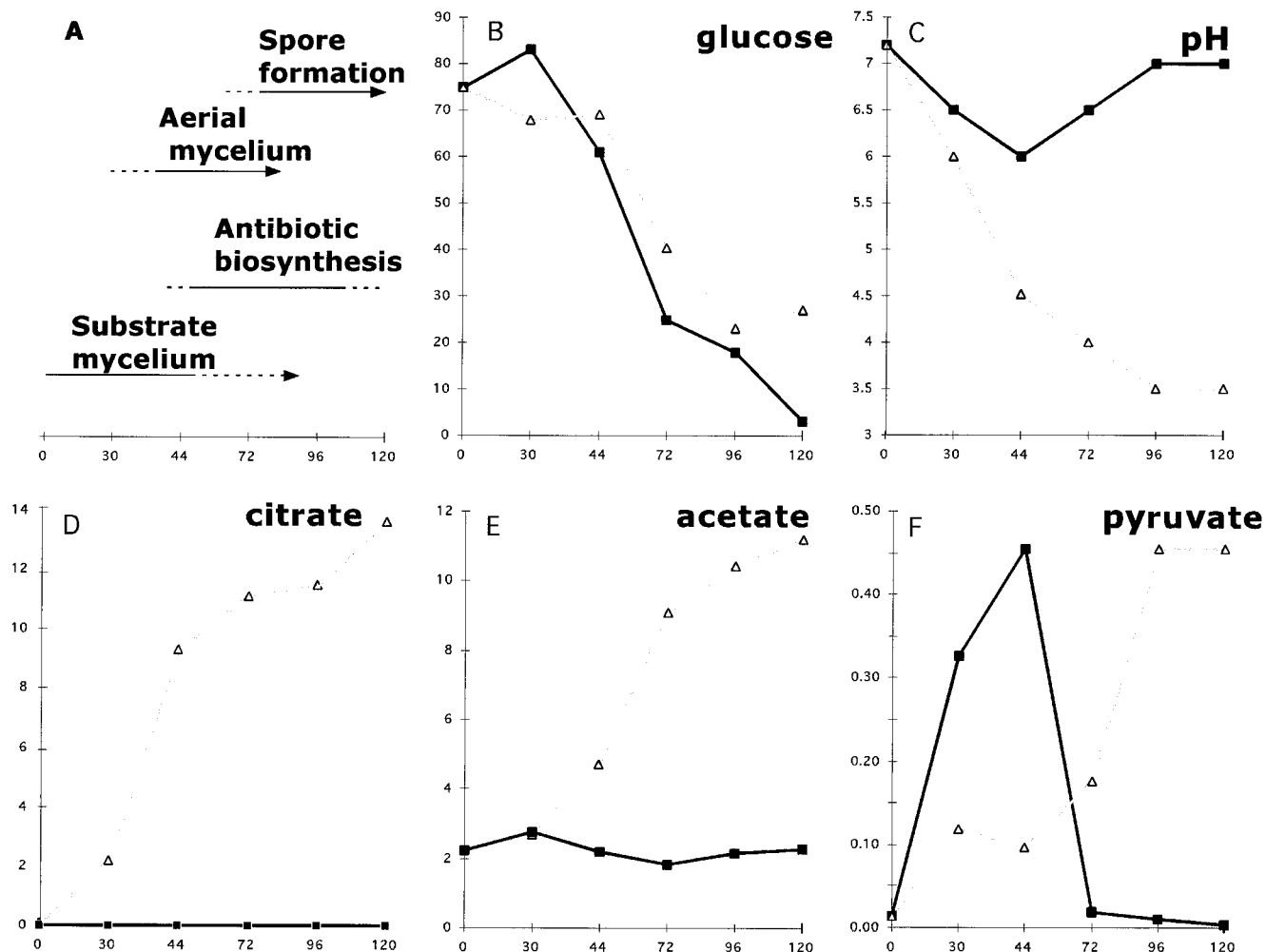


FIG. 3. The developmental block of BZ4 was accompanied by alterations in metabolism. MT1110/pKC1218 (closed squares) and BZ4 (open triangles) were grown on cellophane disks covering R2YE plates (supplemented with 100  $\mu$ g of apramycin/ml to retain the mutant allele). MT1110/pKC1218 underwent typical developmental changes (A) (time in hours is indicated on the x axis), while BZ4 produced neither aerial mycelium nor pigmented antibiotics. An extract of the agar medium was prepared in order to measure pH and metabolite concentrations (glucose, citrate, acetate, and pyruvate were quantified [in millimolar units] as described in Materials and Methods).

cations having diverse activities as cofactors. In addition, the potential toxicity of heavy metals at superoptimal concentrations may complicate efforts to suppress the BZ4 defects by supplementing the medium.

Finally, the fact that the double mutant remained growth impaired relative to both the wild type and *citA* strains on all media tested suggested that AcoA might have an activity independent of its role as an enzyme in the TCA cycle.

***acoA* expression during growth.** Developmentally regulated expression of the *acoA* gene was shown by immunoblot experiments (Fig. 5A) using a polyclonal antibody raised against *E. coli* AcnA to probe protein extracts of MT1110 cultures differentiating on solid R2YE covered by a cellophane membrane. A strongly cross-reacting species migrating with an apparent molecular mass of 97 kDa was detected before white aerial hyphae appeared (Fig. 5A, lane 1). This protein was no longer detected after aerial hypha emergence (Fig. 5A, lanes 2 through 5). While a 97-kDa cross-reactive band was not de-

tected at any time during growth of BZ4, *acoA* mutant extracts (30 h) did contain a cross-reacting band (Fig. 5A, lane 6) that may be a truncation or degradation product of AcoA.

**Mapping the *acoA* promoter in vivo and in vitro.** In order to locate the *acoA* promoter ( $P_{acoA}$ ), a 277-bp *NsiI/XmnI* fragment including 269 bp upstream of the *acoA* translational initiation site was cloned into the promoter probe vector pIJ2839 (pVHP171) (Fig. 6A). This vector allows estimation of promoter activity using a promoterless *xyIE* reporter gene, whose enzyme product can be detected visually or measured enzymatically as a yellow compound (2-hydroxymuconic semialdehyde) (18).

When MT1110/pVHP171 was grown in YEME liquid cultures, XylE (promoter) specific activity increased during early exponential phase (Fig. 5B) and then steadily declined throughout later exponential and stationary phases (XylE may be a rather unstable enzyme [34]). By late stationary phase, the XylE activity reached a minimum value that was >10-fold low-

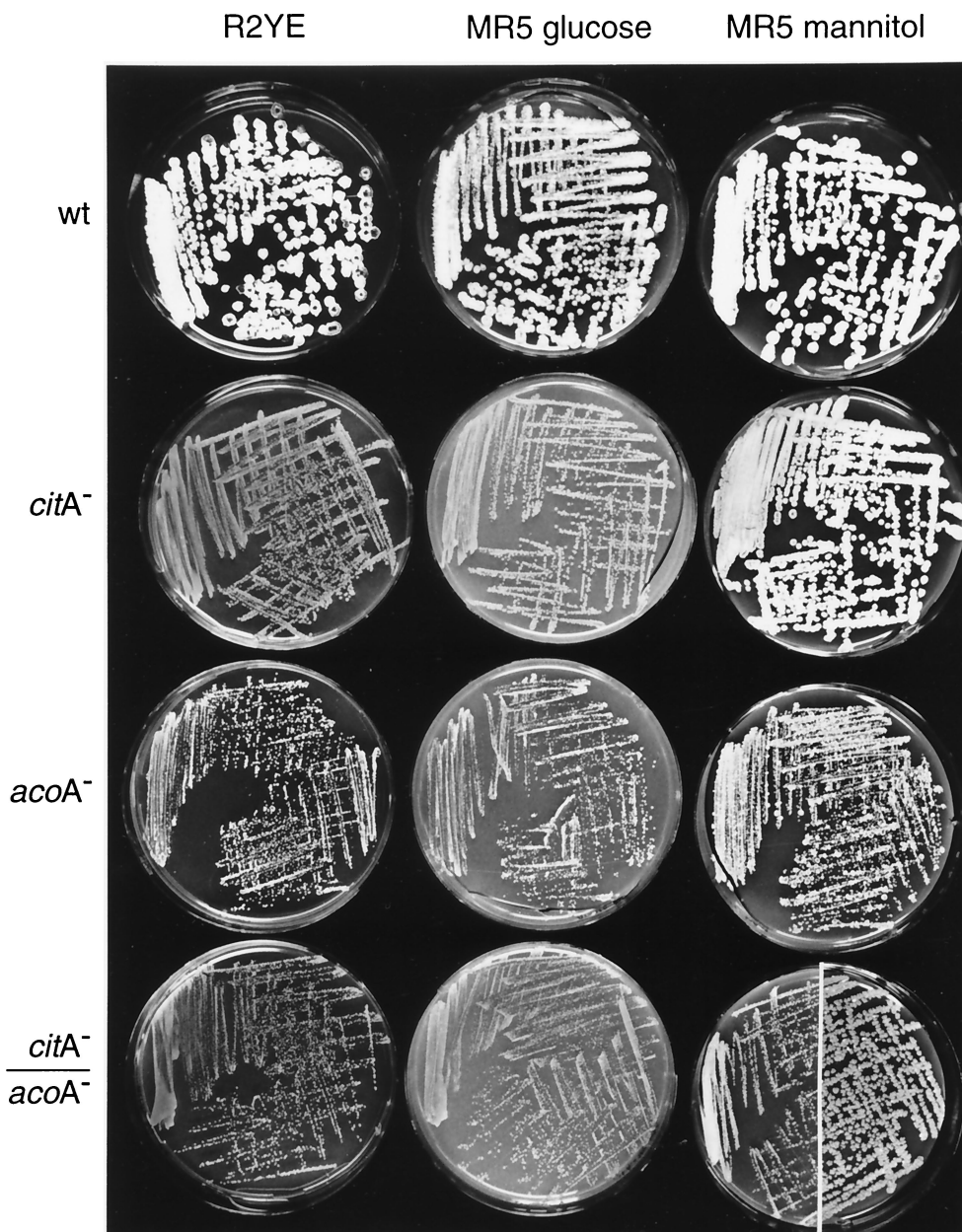


FIG. 4. Colonial phenotypes of TCA cycle mutants. MT1110 (wild type [wt]), BZ2 (*citA*), BZ4 (*acoA*) and BZ5 (*citA acoA*) were streaked out on R2YE or MR5 containing 2% glucose (MR5 glucose) or mannitol (MR5 mannitol). Plates were incubated for 5 days at 30°C and photographed. Colonies had not undergone major changes in morphology upon reexamination 5 days later, with one significant exception. BZ5 colonies had continued to grow and produced gray spores between 5 and 10 days of incubation on MR5 mannitol (photographed and presented as a composite of the right side of the plate).

er (3 mU/mg) than the peak of activity during early exponential phase (27 mU/mg) (34). These experiments indicated that this fragment encoded a promoter activity ( $P_{acoA}$ ).

In order to map the promoter more precisely, primer extension was performed on total RNA isolated from early-exponential-phase cells (12 h) cultivated in YEME. The size of the extended cDNA (157 nucleotides) (Fig. 6C) suggested a transcriptional initiation site located 152 bp upstream of *acoA* (Fig. 6A).

In vitro transcription experiments (Fig. 6B) using a  $P_{acoA}$  template confirmed this transcriptional start site. RNAP iso-

lated from *S. coelicolor* MT1110 grown in YEME to late log phase synthesized an *acoA*-specific mRNA whose size mapped the  $P_{acoA}$  transcriptional start site to the nucleotide found in primer extension experiments (Fig. 6C).

**Extracellular suppression of the *acoA* defect by differentiating wild-type colonies.** When bald BZ4 lawns (high density) or colonies (low density) were grown close to the differentiating wild-type strain (Fig. 2F), they were able to slowly differentiate and produce small amounts of pigment after about a week. The appearance of large suppressor mutant colonies (Fig. 2C, sector 2) hindered the longer-term incubation re-

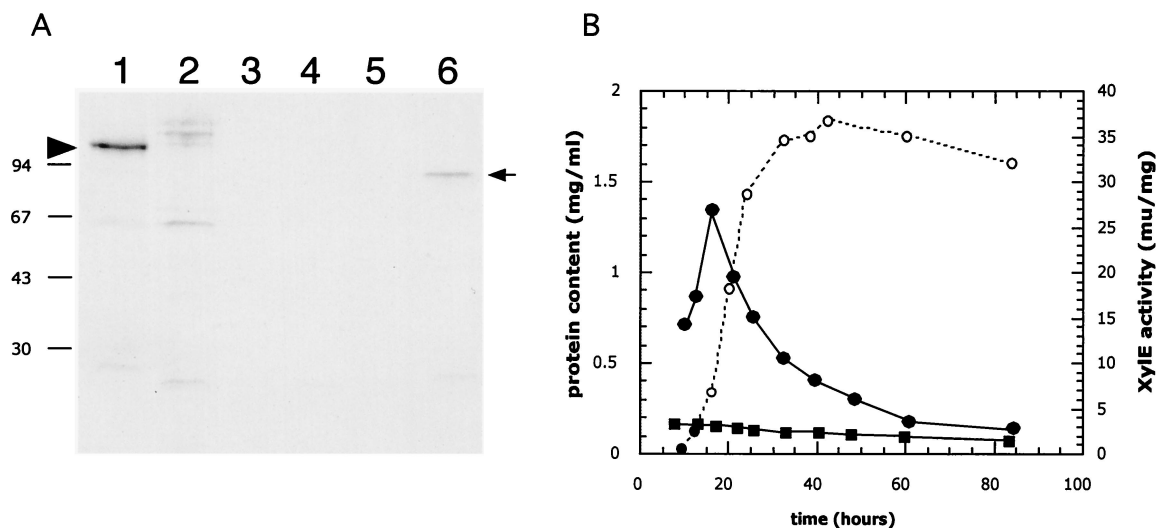


FIG. 5. Developmental control of *acoA*. (A) Accumulation of AcoA in cultures grown on solid medium. AcoA was detected in extracts of surface-grown cultures by immunoblotting using antibodies against *E. coli* AcoA. MT1110/pKC1218 (lanes 1 through 5) and BZ4 (lane 6) were grown on R2YE (containing 100  $\mu$ g of apramycin/ml) plates that had been covered with cellophane disks. Crude extracts prepared from samples harvested after 30 h (lane 1 and 6), 44 h (lane 2), 72 h (lane 3), 96 h (lane 4) and 120 h (lane 5) were resolved by SDS-10% PAGE and transferred to a PVDF nylon membrane. Immunodetection was performed as described in Materials and Methods. The left arrowhead indicates the position of the wild-type AcoA (MT1110/pKC1218), while the arrow on the right points to the presumed truncated or degraded AcoA detected in extracts of BZ4. The molecular masses of the protein marker are indicated on the left (in kilodaltons). (B) Activity of the *acoA* promoter in liquid cultures. *S. coelicolor* MT1110 strains carrying pIJ2839 (a XylE-based promoter probe vector) or a derivative (pVHP171) containing a 277-bp *Nsil/XmnI* fragment (Fig. 6A) extending from within the *acoA* ORF to 269 bp upstream were grown in YEME liquid medium. Crude extracts prepared from cultures throughout growth (open circles, protein content) were assayed for XylE specific activity (closed squares, pIJ2839; closed circles, pVHP171).

quired for "intercolonial complementation" studies of BZ4 with other bald mutants.

## DISCUSSION

The TCA cycle is needed to support both growth and developmental in *B. subtilis* and *S. coelicolor* (8, 19, 42). Sonenshein and his collaborators have proposed that TCA cycle enzymes provide key developmental checkpoints in *B. subtilis*, with aconitase playing an important role. Our studies, as well as those of Schwartz et al. (37), showed that *acoA* mutants have pleiotropic phenotypes, including a defect in development.

Biochemical and genetic studies showed that AcoA was the primary aconitase supporting growth of *S. coelicolor*. Only one activity was observed during column purification of aconitase from liquid-grown mycelial extracts. Expression of *acoA* and accumulation of its product were largely limited to early vegetative growth. Inactivation of the *acoA* gene in BZ4 severely disrupted the TCA cycle activity, clearly indicated by the glutamate auxotrophy of BZ4. This was unlike the *S. viridochromogenes acoA* mutant, which was a prototroph. While the *S. coelicolor* mutant remained bald in the presence of glutamate, the *S. viridochromogenes acoA* mutant was able to produce malformed aerial mycelium (37). These differences probably reflected a second aconitase-like activity able to maintain flux through the TCA cycle in *S. viridochromogenes*. The *S. coelicolor* mutant, devoid of an alternative activity able to support vegetative growth, suffered more severe physiological and developmental defects.

The organic acids (citrate, pyruvate, and acetate) that accumulated to high levels on R2YE media conditioned by the *S.*

*coelicolor acoA* mutant (Fig. 3) inhibited growth via at least two mechanisms. The most obvious inhibition was due to the decrease in pH to levels known to inhibit growth of *S. coelicolor*. As was the case with the *citA* mutant, this effect was partially suppressed by high concentrations of buffer on glucose-based media (Fig. 2). However, the fact that the *acoA* mutant remained growth retarded on these buffered plates as well as on mannitol-based media, in which the pH remained near neutrality, indicated other defects.

In the absence of AcoA, accumulation of its substrate, citrate, was partially responsible for the growth defect of BZ4. The *acoA* growth defects were partially relieved by the *citA* mutation on mannitol-based media, presumably by blocking citrate accumulation (Fig. 4). A mutation in the primary *B. subtilis* aconitase gene similarly resulted in high levels of citrate accumulation and was associated with developmental defects (8). The fact that these defects could be partly suppressed using a quantitative assay for sporulation suggested a model in which chelation of certain divalent cations by citrate was at least partially involved in the developmental phenotype.

A very interesting potential role for AcoA that we have not yet attempted to dissect is in regulating the oxidative stress response. This question has been addressed genetically in other organisms by preventing binding of aconitase to its IRE-like sequences. The ability of AcoA to bind RNA and thus mediate a response to oxidative stress can be preferentially inactivated by a mutagenic change in *B. subtilis* (1). Alternatively, its IRE-like binding sites in upstream untranslated mRNA can be specifically inactivated. Such sites might be identified by searching the *S. coelicolor* genome ([http://www.sanger.ac.uk/Projects/S\\_coelicolor](http://www.sanger.ac.uk/Projects/S_coelicolor)) for its sequence motif (1).

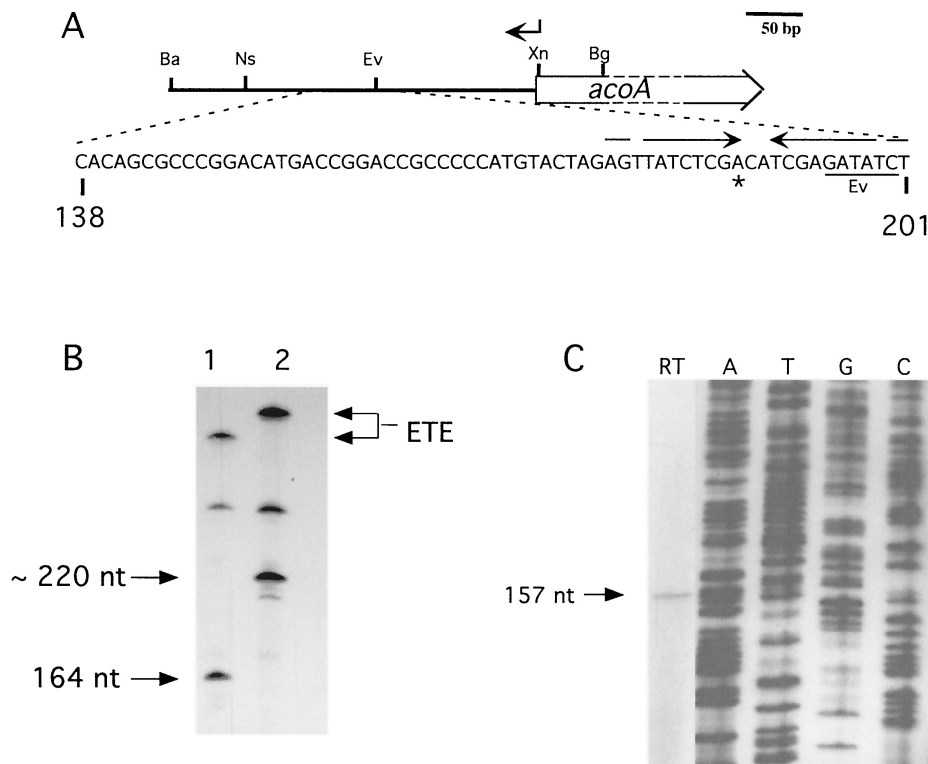


FIG. 6. Mapping the *acoA* transcriptional start site. (A) The *acoA* transcriptional start site locus. Nucleotide coordinates refer to the *acoA* locus sequence. The location of the oligonucleotide used in primer extension is shown by an arrow above the map. Restriction sites: Ba, *Bam*HI; Bg, *Bgl*II; Ev, *Eco*RV; Ns, *Nsi*I; Xn, *Xmn*I. The transcriptional start site (asterisk) mapped in vitro (B) and in vivo (C) was located in a region containing an inverted repeat (opposing arrows). (B) In vitro transcription using two different *acoA* promoter fragments and *S. coelicolor* RNAP. Runoff transcription was carried out using either the 348-bp *Bam*HI/*Xmn*I fragment (lane 1) or the 398-bp *Bam*HI/*Bgl*II fragment (lane 2). The lengths of the two template fragments differed at the *acoA* proximal end, thus fixing the orientation of the runoff transcript. A larger, undefined runoff signal was also obtained from a promoter oriented oppositely to *P<sub>acoA</sub>*. The sizes of the runoff transcripts (arrows on the left) were estimated by separating the samples on a 6% polyacrylamide–6 M urea gel alongside a <sup>32</sup>P-labeled M13mp18 sequencing ladder generated with a standard universal primer (5'-GCCAGGGTTTCCCAGTCACGACG-3'). The signals generated by "end-to-end" (ETE) transcription are indicated on the right. (C) Reverse transcription assay (lane RT) using RNA isolated from exponential-phase *S. coelicolor* grown in YEME. An oligonucleotide overlapping with the *acoA* ORF (coordinates 321 to 344; indicated above by arrow; RT-Aco1 [5'-GACACGACAGTCTCCTTCATTAT-3']) was used as the primer. The size of the cDNA transcript (arrow) was estimated by running the sample alongside a <sup>32</sup>P-labeled M13mp18 sequencing ladder generated with a standard universal sequencing primer (5'-TGTAACGACGGCCAGT-3'; lanes A, T, G, and C).

As in *E. coli*, the *acoA* gene itself may contain an IRE-like sequence in its upstream untranslated region (41) which our data localize to a 152-bp sequence between the transcriptional and translational start sites.

Due to the diverse roles played by aconitase in bacteria, it is difficult to determine whether the defects of the aconitase null mutant reflect its direct role in *Streptomyces* development. Similar questions have been raised in studies of the role of TCA cycle enzymes in the *B. subtilis* sporulation program. Other criteria should be considered to help clarify this question.

Developmental changes correlated well with temporal patterns of *acoA* gene expression. On solid glucose-based R2YE medium, immunoblots demonstrated that AcoA accumulated in early substrate mycelium and then rapidly disappeared later during development as aerial mycelium was formed. Analyses of the underlying physiological or developmental effectors of these regulatory patterns will focus on its promoter region, mapped both in vivo and in vitro to a site 152 bp upstream of the *acoA* ORF. Future studies should clarify why the AcoA protein levels decreased in the colony during aerial mycelium

formation while pyruvate was being consumed (Fig. 3). Catabolism of organic acids may involve TCA oxidation supported by low levels of AcoA or perhaps employ an as-yet-undetected aconitase activity expressed only during aerial mycelial growth (note: *S. viridochromogenes* has at least two aconitase activities [37]). Alternatively, they may be converted to less acidic products, such as lipids or polyketides (42).

Responsiveness to diffusible developmental signals provides the most readily applicable criterion for evaluating whether bald alleles such as *acoA* or *citA* represent an integral part of a programmed differentiation cascade. In *Streptomyces*, differentiation is coordinated by diffusion of well-characterized butyrolactone pheromones (17) and perhaps another positively acting developmental signaling molecule(s) (28, 29, 31, 39, 44, 45). Cultivation of the *acoA* mutants in proximity to the *S. coelicolor* wild type allowed them to differentiate but did not restore normal growth of the colony (Fig. 2F). Therefore, the positive effect of the wild type on differentiation of the *acoA* mutant could reflect such a signal. Alternatively, partial elimination of organic acids or other negatively acting factors by

the wild type might allow BZ4 to form aerial mycelium. Studies of complementation between BZ4 and other acidogenic developmental mutants could in principle provide information to clarify this question; however, frequently arising suppressor strains (as have been observed in *E. coli* [41]) have so far hindered such analyses. Identification of these mutant alleles may provide further insights into the role of *acoA* in development.

Data presented here show that *acoA* is developmentally controlled to support TCA cycle activity during growth of substrate mycelium preceding differentiation. Like citrate synthase mutants (42), *acoA* mutants are TCA cycle arrested, resulting in acidogenesis, glutamate auxotrophy, and disruption of colonial development. Only some of the additional pleiotropic defects of the aconitase mutant could be attributed to citrate accumulation. It is therefore likely that AcoA plays auxiliary roles in growth, perhaps related to iron metabolism or oxidative stress adaptation as reported for *E. coli* (41) and *B. subtilis* (1). These studies, together with our accompanying paper (42), demonstrate the role of TCA cycle enzymes in maintaining metabolic balance, supporting not only growth but also morphologic development and secondary metabolism.

#### ACKNOWLEDGMENTS

We thank John Guest for aconitase antibody, X.-M. Li, J. Vohradsky, and J. Novotna for 2D gel analyses, P. Jenö for N-terminal sequencing, and W. Wohlleben, D. Schwartz, and A. L. Sonenshein for discussions.

This work was supported by Swiss National Science Foundation Grants to C. J. Thompson (3100-039669 and SPP Biotechnology 5002-046085) and W. Minas (SPP Biotechnology 5002-46086).

#### REFERENCES

- Alen, C., and A. L. Sonenshein. 1999. *Bacillus subtilis* aconitase is an RNA-binding protein. *Proc. Natl. Acad. Sci. USA* **96**:10412–10417.
- Bergmeyer, J., and M. Grassl. 1984. *Metabolites. 1. Carbohydrates*. Verlag Chemie, Weinheim, Germany.
- Bierman, M., R. Logan, K. O'Brien, E. T. Seno, R. N. Rao, and B. E. Schoner. 1992. Plasmid cloning vectors for the conjugal transfer of DNA from *Escherichia coli* to *Streptomyces* spp. *Gene* **116**:43–49.
- Bradford, M. M. 1976. A rapid and sensitive method for the quantitation of microgram quantities of protein utilizing the principle of protein-dye binding. *Anal. Biochem.* **72**:248–254.
- Buttner, J. M., and N. L. Brown. 1985. RNA polymerase-DNA interactions in *Streptomyces*: *in vitro* studies of a *S. lividans* plasmid promoter with *S. coelicolor* RNA polymerase. *J. Mol. Biol.* **185**:177–188.
- Buttner, J. M., and N. L. Brown. 1987. Two promoters from *Streptomyces* plasmid pIJ101 and their expression in *Escherichia coli*. *Gene* **51**:179–186.
- Chater, K. F. 1998. Taking a genetic scalpel to the *Streptomyces* colony. *Microbiology* **144**:1465–1478.
- Craig, J. E., M. J. Ford, D. C. Blaydon, and A. L. Sonenshein. 1997. A null mutation in the *Bacillus subtilis* aconitase gene causes a block in Spo0A-phosphate-dependent gene expression. *J. Bacteriol.* **179**:7351–7359.
- Cunningham, L., M. J. Gruer, and J. R. Guest. 1997. Transcriptional regulation of the aconitase genes (*acnA* and *acnB*) of *Escherichia coli*. *Microbiology* **143**:3795–3805.
- Dingman, D. W., M. S. Rosenkrantz, and A. L. Sonenshein. 1987. Relationship between aconitase gene expression and sporulation in *Bacillus subtilis*. *J. Bacteriol.* **169**:3068–3075.
- Doull, J. L., and L. C. Vining. 1989. Culture conditions promoting dispersed growth and biphasic production of actinorhodin in shaken cultures of *Streptomyces coelicolor* A3(2). *FEMS Microbiol. Lett.* **65**:265–268.
- Fouet, A., S. F. Jin, G. Raffel, and A. L. Sonenshein. 1990. Multiple regulatory sites in the *Bacillus subtilis* *citB* promoter region. *J. Bacteriol.* **172**:5408–5415.
- Granozzi, C., R. Billella, R. Passantino, M. Sollazzo, and A. M. Puglia. 1990. A breakdown in macromolecular synthesis preceding differentiation in *Streptomyces coelicolor* A3(2). *J. Gen. Microbiol.* **136**:713–716.
- Gruer, J. M., and J. R. Guest. 1994. Two genetically-distinct and differentially-regulated aconitases (*AcnA* and *AcnB*) in *Escherichia coli*. *Microbiology* **140**:2531–2541.
- Hindle, Z., and C. P. Smith. 1994. Substrate induction and catabolite repression of the *Streptomyces coelicolor* glycerol operon are mediated through the GylR protein. *Mol. Microbiol.* **12**:737–745.
- Hopwood, D. A., M. J. Bibb, K. F. Chater, T. Kieser, C. J. Bruton, H. M. Kieser, D. J. Lydiate, C. P. Smith, J. M. Ward, and H. Schrempf. 1985. *Genetic manipulation of Streptomyces. A laboratory manual*. The John Innes Foundation, Norwich, United Kingdom.
- Horinouchi, S., and T. Beppu. 1994. A-factor as a microbial hormone that controls cellular differentiation and secondary metabolism in *Streptomyces griseus*. *Mol. Microbiol.* **12**:859–864.
- Ingram, M. M., M. Brawner, P. Youngman, and J. Westpheling. 1989. *xyIE* functions as an efficient reporter gene in *Streptomyces* spp.: use for the study of *galPI*, a catabolite-controlled promoter. *J. Bacteriol.* **171**:6617–6624.
- Ireton, K., S. Jin, A. D. Grossman, and A. L. Sonenshein. 1995. Krebs cycle function is required for activation of the Spo0A transcription factor in *Bacillus subtilis*. *Proc. Natl. Acad. Sci. USA* **92**:2845–2849.
- Kelemen, G. H., and M. J. Buttner. 1998. Initiation of aerial mycelium formation in *Streptomyces*. *Curr. Opin. Microbiol.* **1**:656–662.
- Kennedy, C. M., M. H. Emptage, J. L. Dreyer, and H. Beinert. 1983. The role of iron in the activation-inactivation of aconitase. *J. Biol. Chem.* **258**:11098–11105.
- Kretschmer, S. 1982. Dependence of the mycelial growth pattern on the individually regulated cell cycle in *Streptomyces granaticolor*. *Z. Allg. Mikrobiol.* **22**:335–347.
- Laemmli, U. K. 1970. Cleavage of structural proteins during the assembly of the head of bacteriophage T4. *Nature (London)* **227**:680–685.
- MacNeil, D. J. 1988. Characterization of a unique methyl-specific restriction system in *Streptomyces avermitilis*. *J. Bacteriol.* **170**:5607–5612.
- Magni, C., P. Marini, and D. de Mendoza. 1995. Extraction of RNA from gram-positive bacteria. *BioTechniques* **19**:880–884.
- Mazodier, P., R. Petter, and C. Thompson. 1989. Intergeneric conjugation between *Escherichia coli* and *Streptomyces* species. *J. Bacteriol.* **171**:3583–3585.
- Mengaud, J. M., and M. A. Horwitz. 1993. The major iron-containing protein of *Legionella pneumophila* is an aconitase homologous with the human iron-responsive element-binding protein. *J. Bacteriol.* **175**:5666–5676.
- Nodwell, J. R., and R. Losick. 1998. Purification of an extracellular signaling molecule involved in production of aerial mycelium by *Streptomyces coelicolor*. *J. Bacteriol.* **180**:1334–1337.
- Nodwell, J. R., K. McGovern, and R. Losick. 1996. An oligopeptide permease responsible for the import of an extracellular signal governing aerial mycelium formation in *Streptomyces coelicolor*. *Mol. Microbiol.* **22**:881–893.
- Ohne, M. 1974. Regulation of aconitase synthesis in *Bacillus subtilis*: induction, feedback repression, and catabolite repression. *J. Bacteriol.* **117**:1295–1305.
- Onaka, H., T. Nakagawa, and S. Horinouchi. 1998. Involvement of two A-factor receptor homologues in *Streptomyces coelicolor* A3(2) in the regulation of secondary metabolism and morphogenesis. *Mol. Microbiol.* **28**:743–753.
- Pope, K. M., B. D. Green, and J. Westpheling. 1996. The bld mutants of *Streptomyces coelicolor* are defective in the regulation of carbon utilization, morphogenesis and cell-cell signalling. *Mol. Microbiol.* **19**:747–756.
- Rouault, T., and R. Klausner. 1997. Regulation of iron metabolism in eukaryotes. *Curr. Top. Cell Regul.* **35**:1–19.
- Salah-Bey, K., V. Blanc, and C. J. Thompson. 1995. Stress-activated expression of a *Streptomyces pristinaespiralis* multidrug resistance gene (*ptr*) in various *Streptomyces* and *Escherichia coli*. *Mol. Microbiol.* **17**:1001–1012.
- Sambrook, J., E. F. Fritsch, and T. Maniatis. 1989. *Molecular cloning: a laboratory manual*, 2nd ed. Cold Spring Harbor Laboratory, Cold Spring Harbor, N.Y.
- Schuhmann, E., and F. Bergter. 1976. Microscopic studies of *Streptomyces hygroscopicus* growth kinetics. *Z. Allg. Mikrobiol.* **16**:201–205.
- Schwartz, D., S. Kaspar, G. Kienzen, K. Muschko, and W. Wohlleben. 1999. Inactivation of the tricarboxylic acid cycle aconitase gene from *Streptomyces viridochromogenes* Tu494 impairs morphological and physiological differentiation. *J. Bacteriol.* **181**:7131–7135.
- Smokvina, T., P. Mazodier, F. Bocard, C. J. Thompson, and M. Guérouneau. 1990. Construction of a series of pSAM2-based integrative vectors for use in actinomycetes. *Gene* **94**:53–59.
- Süsstrunk, U., J. Pidoux, S. Taubert, A. Ullmann, and C. J. Thompson. 1998. Pleiotropic effects of cAMP on germination, antibiotic biosynthesis, and morphological development in *Streptomyces coelicolor*. *Mol. Microbiol.* **30**:33–46.
- Takano, E., H. C. Gramajo, E. Strauch, N. Andres, J. White, and M. J. Bibb. 1992. Transcriptional regulation of the *redD* transcriptional activator gene accounts for growth-phase dependent production of the antibiotic undecylprodigiosin in *Streptomyces coelicolor* A3(2). *Mol. Microbiol.* **6**:2797–2804.
- Tang, Y., and J. R. Guest. 1999. Direct evidence for mRNA binding and post-transcriptional regulation by *Escherichia coli* aconitases. *Microbiology* **145**:3069–3079.
- Viollier, P. H., W. Minas, G. E. Dale, M. Folcher, and C. J. Thompson. 2001. Role of acid metabolism in *Streptomyces coelicolor* morphological development and antibiotic biosynthesis. *J. Bacteriol.* **183**:3184–3192.

43. **Vohradsky, J., X. M. Li, and C. J. Thompson.** 1997. Identification of pro-caryotic developmental stages by statistical analyses of two-dimensional gel patterns. *Electrophoresis* **18**:1418–1428.
44. **Willey, J., R. Santamaria, J. Guijarro, M. Geistlich, and R. Losick.** 1991. Extracellular complementation of a developmental mutation implicates a small sporulation protein in aerial mycelium formation by *S. coelicolor*. *Cell* **65**:641–650.
45. **Willey, J., J. Schwedock, and R. Losick.** 1993. Multiple extracellular signals govern the production of a morphogenetic protein involved in aerial mycelium formation by *Streptomyces coelicolor*. *Genes Dev.* **7**:895–903.
46. **Wilson, T. J., N. Bertrand, J. L. Tang, J. X. Feng, M. Q. Pan, C. E. Barber, J. M. Dow, and M. J. Daniels.** 1998. The *rpfA* gene of *Xanthomonas campestris* pathovar *campestris*, which is involved in the regulation of pathogenicity factor production, encodes an aconitase. *Mol. Microbiol.* **28**:961–970.